Jpn. J. Appl. Phys. Vol. 40 (2001) pp. 3320–3325
Part 1, No. 5A, May 2001

Mechanical Properties of Phase-change Recording Media: GeSbTe Films

Chao-An JONG, Weileung FANG[1], Chain-Ming LEE and Tsung-Shune CHIN*

Department of Materials Science and Engineering, National Tsing Hua University, 101, Sec. 2, Kuang-Fu Road, Hsinchu 30043, Taiwan, R.O.C
[1]*Department of Power Mechanical Engineering, National Tsing Hua University, 101, Sec. 2, Kuang-Fu Road, Hsinchu 30043, Taiwan, R.O.C*

(Received September 18, 2000; accepted for publication January 9, 2001)

Mechanical properties of as-deposited GeSbTe media on SiO_2/Si(100) with different compositions and film thicknesses were successfully investigated by using the microcantilever method and nanoindentation. All the studied films show a compressive residual stress state, which increases proportionally to the elastic constant. Because of the accumulating effects during film deposition, the mechanical properties of these GeSbTe films can be greatly affected. As the film thicknesses were 20 and 25 nm, compared with the Ge_4SbTe_5 and $Ge_4Sb_{0.5}Te_5Bi_{0.5}$ films, the $Ge_2Sb_2Te_5$ film has the highest residual stress value ranging from 3 MPa to 15 MPa. When the film thickness was 30 nm, the composition-induced stress relaxation occurred. Bi addition, which leads to lattice expansion in Ge_4SbTe_5 films, resulted in a decrease of stress. Compared with the Ge_4SbTe_5 and $Ge_4Sb_{0.5}Te_5Bi_{0.5}$ films, the $Ge_2Sb_2Te_5$ film also has the lowest coefficient of thermal expansion (CTE) value ranging from 2×10^{-6} to 7×10^{-6}/°C, and a lower CTE was obtained when the film thickness was increased. By nanoindentation, the Ge_4SbTe_5 film shows higher hardness and elastic constant than those of the $Ge_2Sb_2Te_5$ film. The measured hardnesses for $Ge_2Sb_2Te_5$ and Ge_4SbTe_5 films are 12 GPa and 18 GPa; and the reduced elastic modului are 120 GPa and 140 GPa, respectively.

KEYWORDS: mechanical properties of thin films, phase-change recording media, GeSbTe films, residual stress, coefficient of thermal expansion, elastic modulus, hardness

1. Introduction

Recently, with the requirement of high recording density, the application of optical technique in data storage has attracted much attention. The magneto-optical (MO) disk and the phase-change optical recording disk have been widely studied, and both have been commercially available, such as the 230 MByte MO disk, 650 MByte compact disc rewritable (CD-RW), and 4.7 GByte digital versatile disk (DVD) disks.

Because of some potential advantages superior to those of MO recording, phase change optical recording is one of the promising techniques for data storage. Among phase-change materials, media based on the mixture of GeTe–Sb_2Te_3 with high crystallization speed and thermal-stability have become the most widely adopted materials. Among them the three ternary compounds—$GeSb_4Te_7$, $GeSb_2Te_4$, and $Ge_2Sb_2Te_5$—standing in a row on the pseudo-binary tieline connecting GeTe and Sb_2Te_3, have been extensively studied. These compounds perform very fast (on the order of 10^{-6} s) transformation between amorphous and crystalline phases, contributing to the advantages of high-speed writing and erasing in the laser heating recording processes. Therefore, the performance of the disk will be dependent on thermal behaviors of the media. The effects of additional elements on promoting optical contrast and crystallization temperature have also been studied.[1,2] A $Ge_4Sb_{0.5}Te_5Bi_{0.5}$ film has been reported to have an excellent carrier to noise (CNR) ratio ($>$ 50 dB) and cyclability ($> 10^5$).[3] However, very few studies, to the acknowledgement of the present authors, have been devoted to thermal and mechanical properties of GeSbTe based film, such as the $Ge_2Sb_2Te_5$, Ge_4SbTe_5 and $Ge_4Sb_{0.5}Te_5Bi_{0.5}$. They were thus selected and studied in this work.

Different from the average data obtained from a film on a full wafer for stress and coefficient of thermal expansion (CTE), specific data obtained from a local area were explored by a microcantilever prepared by the micro-electro-mechanical-system (MEMs) technique. The sensing load-displacement nanoindentation technique was used for the hardness and elastic modulus measurements.

2. Experimental Procedures

According to requirements for different measurements, the SiO_2 single layer cantilever beams prepared by the MEMs technique were used to deposit films for stress and CTE measurements, and films on bare silicon wafers for nanoindentation experiments.

2.1 Formation of cantilever beams

In this study, the bi-layer cantilever beam method was adopted to determine the residual stress and CTE. Silicon dioxide (SiO_2) films were thermally grown on p-type Si (100) substrates, which were cleaned previously by dipping into HF solution and acetone and then rinsed in distilled water. After spin-drying and baking at 150°C for 30 min, the oxides were prepared by a dry oxygen method in a conventional furnace at 1050°C. After oxidation, the thickness was examined using nanospectrometry (AFT model-210, NANOSPEC) and determined to be around 1.04 μm on average. Nanospectrometry is a useful instrument for various materials used in VLSI processing, especially for some oxides, nitrides and polysilicon film, such as the thermal-SiO_2 by oxidation, the SiO_2 by chemical vapor deposition, and polysilicon by low pressure chemical vapor deposition (CVD). Prior to the measurement, the optical property database such as the refractive index should be established.

For the film thickness measurement, a suitable optical properties database of the desired material that was prepared by the same procedures should be chosen. Then, in comparison with the interference fringes of the composite structure (film/silicon wafer) and bare silicon wafer, the film thickness can be obtained by computer program calculation. It is convenient for thickness measurement of thicker films with deviation within the range ±10 nm.

---

*Corresponding author. E-mail: tschin@mse.nthu.edu.tw

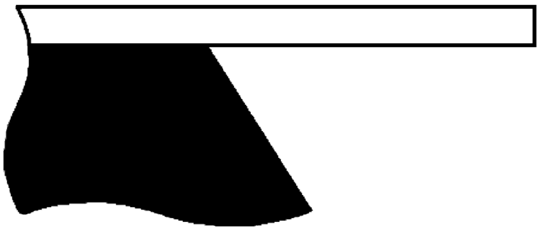

(a)

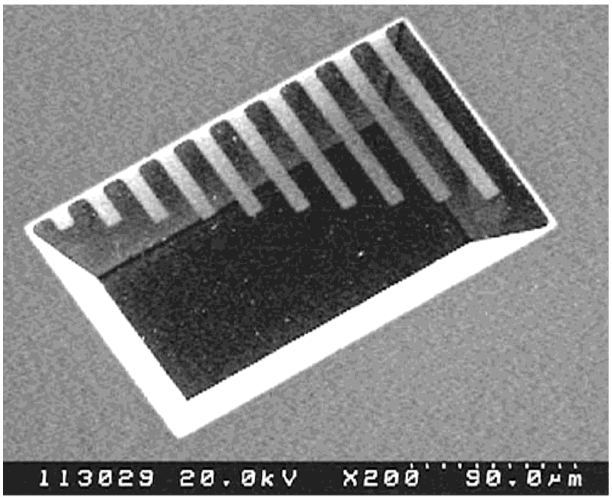

(b)

Fig. 1. (a) Schematic and (b) SEM photograph of as-formed SiO_2 cantilever beams after removal of Si membrane.

In order to produce micro-cantilever beams, the oxide and the silicon substrates must be patterned and etched. By way of lithography, the oxides were patterned into some testing structure, and due to the etching selectivity between silicon and oxide, the silicon under-layer was etched using 15 wt% KOH solutions at 80–85°C for 30 min. The cantilever beams with fixed width of 10 μm and different lengths were formed, and the beam of length 100 μm was arbitrarily chosen for the observation of interference fringes (Fig. 1); since the parameters measured by the interferometer, deflection and curvature of the beams, were not functions of the beam length. That is to say, the deviations among results for beams of different lengths are negligible. Thus, by taking the average of the data measured from different dies on the same wafer, the deviation could be minimized.

2.2 Thin film deposition

The $Ge_2Sb_2Te_5$, Ge_4SbTe_5 and $Ge_4Sb_{0.5}Te_5Bi_{0.5}$ films were prepared by RF magnetron sputtering onto (100) silicon and SiO_2 cantilever beams by using a commercial $Ge_2Sb_2Te_5$ target, Ge_4SbTe_5 target, and a composite Ge_4SbTe_5 target (all targets from Mitsubishi Materials Co.) with different area ratios of Bi chips on them. The background pressure was below 9×10^{-7} Torr and the rf power was 37 W. Films of three different thicknesses—20 nm, 25 nm, and 30 nm—were prepared at room temperature for microcantilever beam study, and 200 nm films for nanoindentation study. A Tencor 250 (α-step) profiler was used to check the thickness of all GeSbTe films.

2.3 Measurement of mechanical properties

The residual stress and the CTE were obtained by measuring the radius of curvature of the deflected micro-beams using an optical interferometer. The heating procedure was performed within a chamber with a constant heating rate (1°C/min), which will not cause any thermal damage, up to 100°C, and the temperature deviation was kept within ±0.1°C for 2 min. The deflection of the micro-beams and the boundary rotation angle (θ) were recorded simultaneously. Using a personal computer the shifts in interference fringes due to the deformation of the beam were recorded, and the change in radius of curvature can be obtained.

An improved nano-indentation system (Triboscope$^{\text{TM}}$, Hysitron) was used to measure the reduced elastic modulus (E_r) and hardness (H) of the films. The instrument continuously records both indentation loads and displacement, and from these data it is possible to derive a variety of mechanical properties. Here, a Berkovich diamond indenter, a triangular pyramid diamond whose depth-area relationship is the same as that of a Vickers indenter, with $E_{\text{diamond}} = 1,141$ GPa and $v_{\text{diamond}} = 0.07$ was used. The resolutions of load and displacement were less than 1 nN and 0.0002 nm, respectively.

3. Results and Discussion

3.1 Residual stress analysis

Combining the intrinsic strain due to the mismatch of two different films and thermal strain, the total strain of the bilayer beam derived by Timoshenko was simplified as follows:

$$\epsilon_{\text{total}} = \frac{\left[(r_2 - r_1) \times \frac{t_{\text{film}}}{2}\right] + (r_2 - r_1) \times \frac{E_B(t_{\text{film}} + t_B)}{2(E_{\text{film}} + E_B)}}{r_1 r_2 + \frac{r_1 t_{\text{film}}}{2} + r_1 \times \left[\frac{E_B(t_{\text{film}} + t_B)}{2(E_{\text{film}} + E_B)}\right]} \tag{1}$$

$$\epsilon_{\text{film}} = \epsilon_{\text{total}} - \epsilon_{\text{oxide}}. \tag{2}$$

Thus, the residual stress which was a function of E_{film} can be calculated by the formula:

$$\sigma_f = f(E_{\text{film}}) = E_{\text{film}} \epsilon_{\text{film}}. \tag{3}$$

Here, E_{film}, t_{film} and E_B and t_B are the elastic modulus and thickness of the GeSbTe film and SiO_2 substrate, respectively. r_1 and r_2 are the radius of curvature for the single and bilayer beam, respectively, and both are calculated from the curvature center to the neutral axis.

In this study, E_{film}, the elastic modului of films studied in this work, are taken as arbitrary values between 50 and 250 GPa. Herein, the test structure was designed as an array all over the 5-inch mask, the final data is the average result measured from different dies of the same wafer. The deviation of the measured stress data was ±0.25 MPa, which may have originated from the defocusing fringes of the interferometer. Figure 2 shows the residual stresses of studied films with different thicknesses varying from 20 nm to 30 nm for the films of $Ge_2Sb_2Te_5$, Ge_4SbTe_5 and $Ge_4Sb_{0.5}Te_5Bi_{0.5}$ films. All the

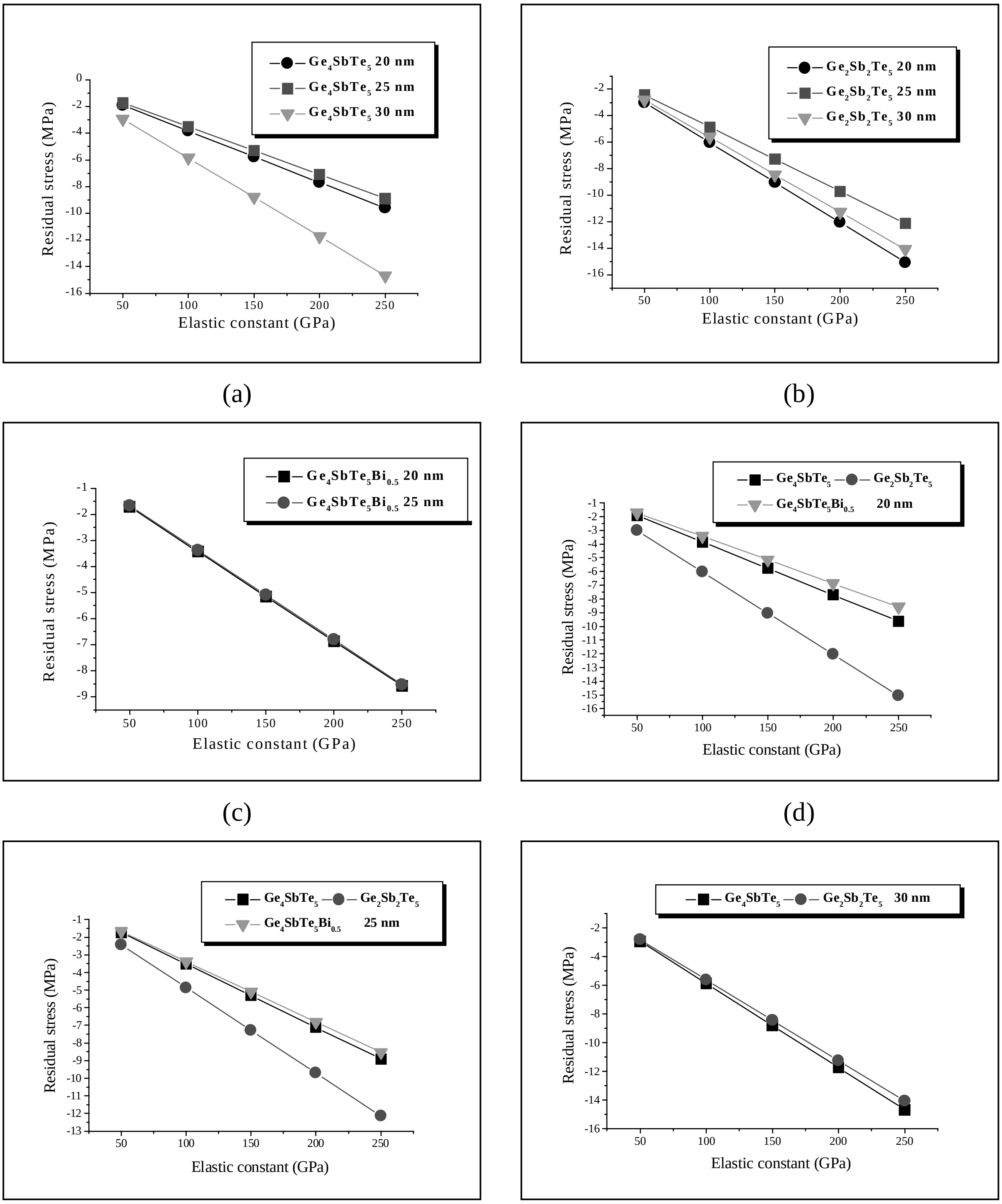

(a) (b) (c) (d) (e) (f)

Fig. 2. The dependence of residual stress on assumed elastic constants of the GeSbTe films with different thicknesses: (a) Ge_4SbTe_5 film, (b) $Ge_2Sb_2Te_5$ film, and (c) $Ge_4Sb_{0.5}Te_5Bi_{0.5}$ films; and GeSbTe films of fixed thickness (d) 20 nm (e) 25 nm and (f) 30 nm.

films after deposition exhibit a compressive residual stress increasing proportionally to the elastic constant which varies from 1.5 MPa to 15 MPa. The residual stress varies with film thickness in the sequence of 30 nm $>$ 20 nm $>$ 25 nm for Ge_4SbTe_5 films, and 20 nm $>$ 30 nm $>$ 25 nm for $Ge_2Sb_2Te_5$ films. When the film thickness was 25 nm, both the Ge_4SbTe_5 and $Ge_2Sb_2Te_5$ films had the lowest residual stress. According to the write-testing results$^{4)}$ of the as-deposited four-layer structure: PC substrate/(130 nm) $ZnS–SiO_2$/(20,25,30 nm) $Ge_{21}Sb_{26}Te_{53}$/(36 nm) $ZnS–SiO_2$/(90 nm) Al, the CNR value at 25 nm thickness was nearly 50 dB better than that of 20 and 30 nm films, and proved to have the desired noise level results as revealed thermal simulation. This value also meets the requirements of commercial disks (45 dB). This result provides proof of the importance of the as-deposited residual stress state on the disk performance. On the other hand, in view of close-packed structure for GeSbTe glass (or amorphous films), due to the higher coordination number for Ge ($Z = 4$) than Sb ($Z = 3$), the short-range microstructure of the Ge-dominated film is organized by cross-linking network

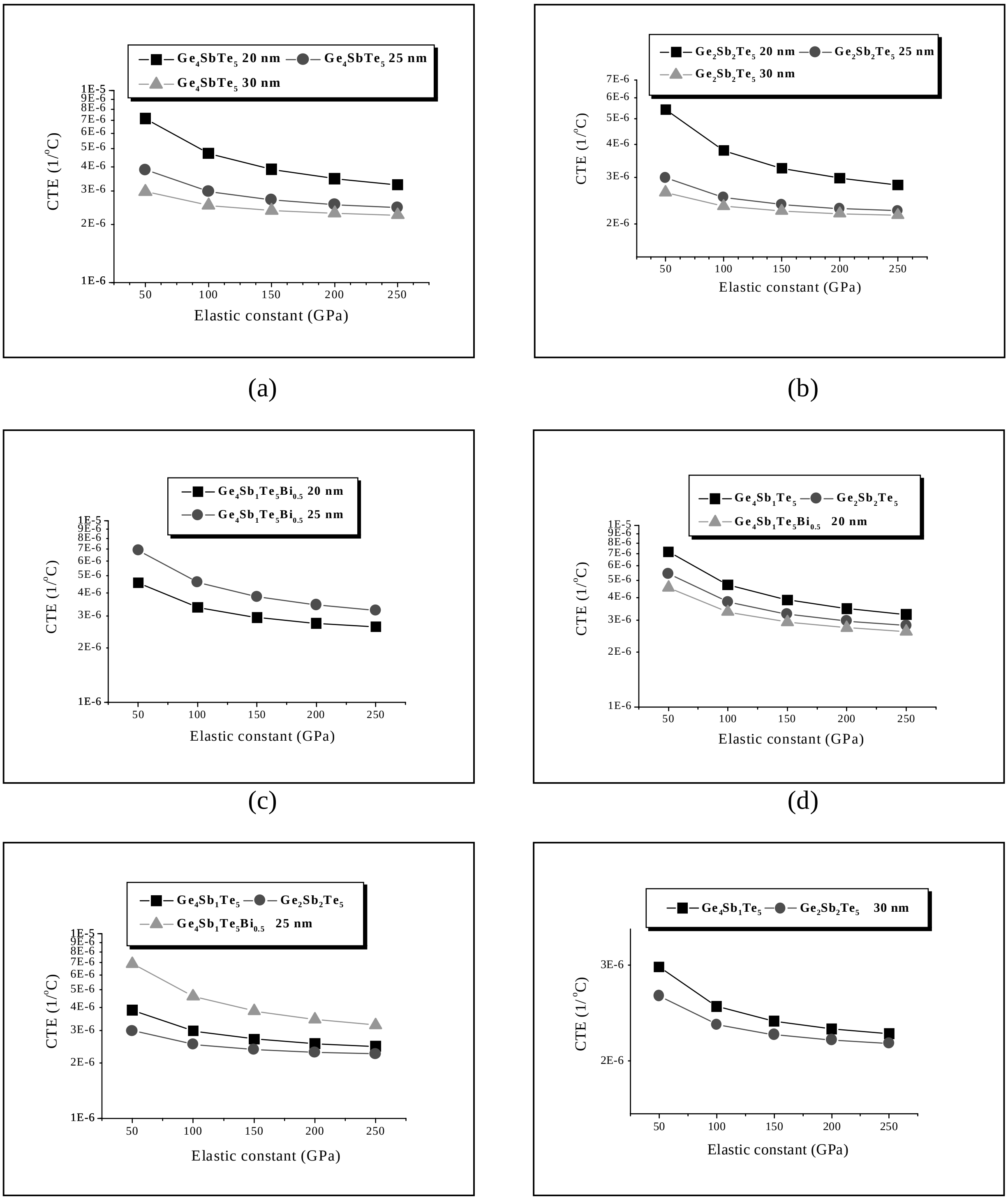

(a) (b) (c) (d) (e) (f)

Fig. 3. The dependence of CTE on assumed elastic constants of the GeSbTe films with different thicknesses: (a) Ge_4SbTe_5 film, (b) $Ge_2Sb_2Te_5$ film, and (c) $Ge_4Sb_{0.5}Te_5Bi_{0.5}$ films; and GeSbTe films of fixed thickness (d) 20 nm (e) 25 nm and (f) 30 nm.

that is different from the mostly branching structure in the Sb-dominated film.[5)] Hence, the effect of film composition on microstructure, as well as the residual stress, CTE and the hardness is believed to arise from the bonding structural difference with respect to the cross-linking network and branching in the amorphous packing. For $Ge_4Sb_{0.5}Te_5Bi_{0.5}$ films, film thickness seems to have no obvious effect on the value of residual stress ranging from 1.5 MPa to 8.5 MPa as shown in Fig. 2(c).

When the film thickness was kept constant, the comparisons of residual stresses among these three films are shown in Figs. 2(d)–2(f). Among them, the $Ge_4Sb_{0.5}Te_5Bi_{0.5}$ films usually have the lowest residual stresses that are slight lower than those of Ge_4SbTe_5 films. This indicates the Bi addition effect on residual stress is negligible. Furthermore, at the thicknesses of 20 nm and 25 nm, the Ge_4SbTe_5 films have lower residual stresses than those of $Ge_2Sb_2Te_5$ films. When the film thickness is 30 nm, the reverse is true. Ovshinsky[6)] claimed that a face-center cubic (fcc) structure is formed by adding Sb atoms to substitute Ge atoms, and

Table I. The calculated residual stresses (σ) and CTE values of Ge_4SbTe_5 and $Ge_2Sb_2Te_5$ films of different thicknesses (t). The elastic constants are calculated from reduced elastic constant from the nanoindentation method using eq. (7) assuming the Poisson ratios of 0.25 and 0.35.

		Ge_4SbTe_5 films		$Ge_2Sb_2Te_5$ films	
Poison ratio (υ)		$\upsilon = 0.25$	$\upsilon = 0.35$	$\upsilon = 0.25$	$\upsilon = 0.35$
Elastic constant		123.2 GPa	131.6 GPa	105.6 GPa	112.8 GPa
σ (MPa)	$t = 20$ nm	4.9	5.2	6.3	6.8
	$t = 25$ nm	4.4	4.7	5.1	5.6
	$t = 30$ nm	7.2	7.8	5.9	6.4
CTE (10^{-6}/°C)	$t = 20$ nm	4.3	4.1	3.8	3.6
	$t = 25$ nm	2.9	2.7	2.5	2.4
	$t = 30$ nm	2.4	2.3	2.4	2.3

the internal stress of the GeTe structure seems to be relaxed. Only at 30,nm, the effect of substituting Ge by Sb ($Ge_4SbTe_5 \rightarrow Ge_2Sb_2Te_5$), the residual stresses will be relaxed, that is $\sigma_{Ge_4SbTe_5} > \sigma_{Ge_2Sb_2Te_5}$, which agrees with the results of Ovshinsky. Here, the measured residual stress is composed of the intrinsic stress and the thermal stress. The intrinsic stress originates from the accumulating effect of the crystallographic flaws that are built into the coating during deposition and plasma heating during film deposition, respectively. Thus, not only the composition but also the film thicknesses can affect the residual state of GeSbTe films.

In Figs. 2(d) and 2(e), the $Ge_4Sb_{0.5}Te_5Bi_{0.5}$ films usually have lower residual stresses than the Ge_4SbTe_5 films. We believe that the lattice expansion by adding larger Bi atoms to substitute smaller Sb atoms will decrease the compressive stress.

3.2 CTE

The difference in CTE ($\Delta\alpha_f = \alpha_{oxide} - \alpha_{film}$) introduced by the temperature change (ΔT) from room temperature to 100°C was calculated by the relationship between the change of radius of curvature ($= \Delta(1/\rho)$) of the bilayer beam:

$$\Delta\left(\frac{1}{\rho}\right) = \frac{6 \cdot \Delta T \cdot \Delta\alpha_f \cdot (1+m)^2}{h \cdot [3 \cdot (1+m)^2 + (1+m \cdot n)(m^2 + m \cdot n)]} \tag{4}$$

Where h is the total thickness of the bilayer beam ($= h_{Oxide} + h_{film}$), $n = E_{oxide}/E_{film}$ and $m = h_{Oxide}/h_{film}$. Figure 3 shows the CTE values varying with elastic constant and film thickness. All the values decrease rapidly at lower elastic constant and approach a constant value gradually as the elastic constant above 200 GPa. Furthermore, the greater of the film thickness the smaller the CTE value. It is generally accepted that a microstructurally cross-linked film (less defects such as porosity) has a lower CTE value than that of a branching one. As the film thickness increases, the voids will be filled and minimized; the CTE values will thus decrease. This maybe the reason why the thicker Ge_4SbTe_5 film 30 nm has larger residual stress than the $Ge_2Sb_2Te_5$ films. The Ge_4SbTe_5 films usually have higher CTE value than $Ge_2Sb_2Te_5$ films independent of film thickness in this study. We think that the Ge-rich network (Ge_4SbTe_5 films) randomly stacked during film deposition will become less-dense than those of Sb-rich films ($Ge_2Sb_2Te_5$ films) when the film thickness is less than 25 nm.

The CTE comparison of these three films when the film thickness was kept constant is also shown in Figs. 3(d)–3(f). The effect of Bi addition for the Ge_4SbTe_5 film and the $Ge_4Sb_{0.5}Te_5Bi_{0.5}$ film at 20 and 25 nm is opposite. This is due to the opposite thermal expansion behavior for Bi. The effect is more significant for thicker films. The CTE is more important than residual stress in disk performance. Furthermore, the CTE changes markedly at a low elastic constant (< 150 GPa) and approaches a constant value at a high elastic constant (> 200 GPa). If the thickness or elastic constant (film composition) can be well controlled, this will improve the performance of optical disk.

In this study, Bi-modified GeSbTe film ($Ge_4Sb_{0.5}Te_5Bi_{0.5}$ film) was compared with the other two films in terms of residual stress and CTE data. The $Ge_4Sb_{0.5}Te_5Bi_{0.5}$ film, which exhibits lower stress, CTE, and excellent cyclability ($> 10^5$), is a suitable candidate as the optical recording medium. In order to decrease the laser-induced damage, matching of CTE values is essential among the four layers disk structure: GeSbTe film, the lower dielectric film, the upper dielectric film, the reflection layer and the substrate.

3.3 Hardness and elastic properties

Figures 4 and 5 are the measured hardness and reduced elastic modulus (E_r) vs displacement curves for $Ge_2Sb_2Te_5$ and Ge_4SbTe_5 films, respectively. In order to obtain the intrinsic mechanical properties of thin films, it is generally accepted that the indentation displacement (h) to be measured should be less than 1/10 of the film thickness. If the displacement is greater than 1/10 of the film thickness, the measured properties (the hardness and the elastic constants) would be contributed from the substrate as well. That is to say, the effect of substrate should not be ignored. In this study, the intrinsic film property is shown at a low depth (small load) when the indentation depth is less than 20 nm, approximately 1/10 that of film thickness (200 nm).

According to Pharr and Oliver's formulas[7] the hardness and E_r can be expressed by:

$$\frac{dP}{dh} = \frac{2}{\sqrt{\pi}} E_r \sqrt{A} \tag{5}$$

$$H = \frac{P_{max}}{A} \tag{6}$$

$$\frac{1}{E_r} = \frac{1-(\upsilon_{film})^2}{E_{film}} + \frac{1-(\upsilon_{diamond})^2}{E_{diamond}} \tag{7}$$

where P: applied load h: relative displacement, A: projected area of impression as a function of hc, $A = A(h_c)$ h_c: *in-situ* contact depth E_r: reduced elastic modulus.

According to the data in Figs. 4 and 5, as a fixed load is applied, the $Ge_2Sb_2Te_5$ film shows larger displacement than that

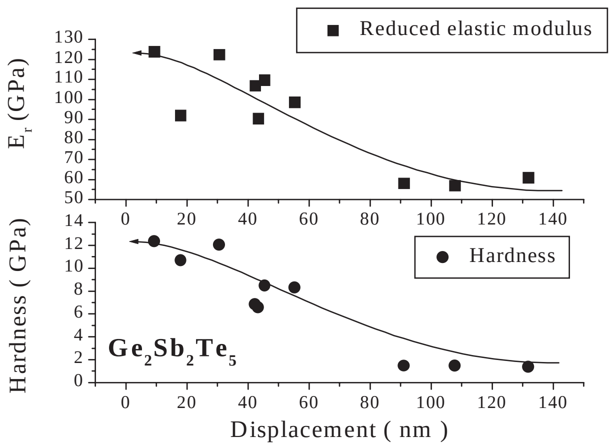

Fig. 4. The dependence of hardness and reduced elastic constant on indentation displacement for a $Ge_2Sb_2Te_5$ film.

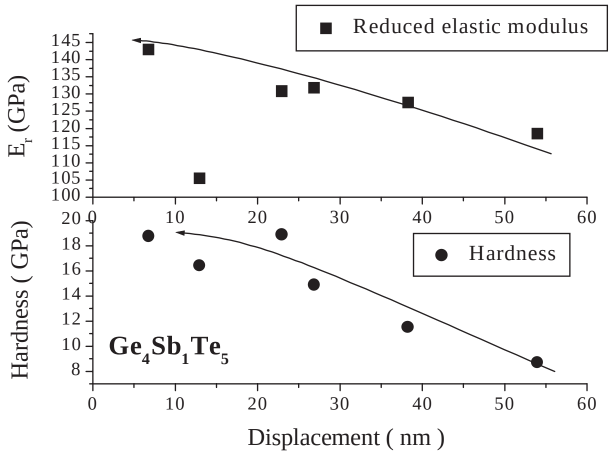

Fig. 5. The dependence of hardness and reduced elastic constant on indentation displacement for a Ge_4SbTe_5 film.

of the Ge_4SbTe_5 films, and the difference is manifested further at small loads. That is to say, the Ge_4SbTe_5 film is harder than the $Ge_2Sb_2Te_5$ film. According to the stress analysis, the Sb-rich film (such as $Ge_2Sb_2Te_5$ films) seems to be denser than Ge_4SbTe_5 films. The Ge-rich film (Ge_4SbTe_5 film) exhibits a more complex bonding structure than the Sb-rich film ($Ge_2Sb_2Te_5$ films), and shows higher resistance to indentation than does the $Ge_2Sb_2Te_5$ films. The hardness at displacement of less than 20 nm is about 18 GPa for the Ge_4SbTe_5 film and 12 GPa for the $Ge_2Sb_2Te_5$ film. On the other hand, the reduced elastic modului for Ge_4SbTe_5 and $Ge_2Sb_2Te_5$ films are 140 GPa and 120 GPa, respectively.

Since the Poisson ratio (υ) of materials is smaller than 0.5 (usually around 0.3), and the diamond term in E_r calculation is usually ignored, it is manifested that the real elastic modului of these two films are close to yet slightly smaller than the measured E_r values. For instance assuming the unknown υ value of the film is within 0.25 to 0.35, eq. (7) gives an E_{film} value of $0.88E_r$ to $0.94E_r$. That is to say, the true elastic constant is $123.2\,\text{GPa} < E_{\text{film},415} < 131.6\,\text{GPa}$ for Ge_4SbTe_5 film, and $105.6\,\text{GPa} < E_{\text{film},225} < 112.8\,\text{GPa}$ for $Ge_2Sb_2Te_5$ film as the υ value is within 0.25 to 0.35. The residual stresses and CTE values calculated in this study were also obtained and are summarized in Table I.

4. Conclusions

In this study, the mechanical properties of three GeSbTe ($Ge_2Sb_2Te_5$, Ge_4SbTe_5, $Ge_4Sb_{0.5}Te_5Bi_{0.5}$) films were investigated by using the microcantilever and nanoindentation method. The data obtained are reported for the first time. Different from the average data obtained by the conventional full-wafer method, the data of the microcantilever beam method is useful to calculate the local residual stresses and coefficient of thermal expansion (CTE) values.

All the studied films deposited on Si (100) show compressive residual stress that is proportional to the elastic constant. In view of the close-packed structure for GeSbTe glass (or amorphous films), due to higher coordination number for Ge ($Z = 4$) than Sb ($Z = 3$), the short-range microstructure for the Ge-dominated film was organized by cross-linked network that is different from the branching Sb-dominated film. Hence, the effect of film composition on microstructure, as well as the residual stress, CTE and the hardness are discussed. The stress of the $Ge_2Sb_2Te_5$ film is greater than that of the Ge_4SbTe_5 film except for the film thickness of 30 nm, which originated from the composition effect. The Bi addition to substitute half of the Sb in Ge_4SbTe_5 films can effectively lower the stress of the Ge_4SbTe_5 film for the film thicknesses of 20 and 25 nm.

All the coefficient of thermal expansion values of the $Ge_2Sb_2Te_5$ films are smaller than those of the Ge_4SbTe_5 films for the various thicknesses considered. According to the stress analysis, the $Ge_2Sb_2Te_5$ film is microstructurally denser than the Ge_4SbTe_5 film; the result is also manifested in CTE analysis. As the film thickness increases, the voids will be minimized and the CTE values will thus decrease. For both $Ge_2Sb_2Te_5$ and Ge_4SbTe_5 films, the CTE values are inversely proportional to the film thickness.

For hardness and elastic property measurement, the Ge_4SbTe_5 film shows higher hardness and elastic modulus than those of the $Ge_2Sb_2Te_5$ film. The measured hardnesses for $Ge_2Sb_2Te_5$ and Ge_4SbTe_5 films are 12 GPa and 18 GPa; and the reduced elastic constants are 120 GPa and 140 GPa, respectively. With a reasonable assumption of the υ value of 0.25 to 0.35, the elastic constants are $123.2\,\text{GPa} < E_{\text{film},415} < 131.6\,\text{GPa}$ and $105.6\,\text{GPa} < E_{\text{film},225} < 112.8\,\text{GPa}$ for the Ge_4SbTe_5 and $Ge_2Sb_2Te_5$ films, respectively.

Acknowledgment

The authors would like to thank the National Science Council of the Republic of China for the financial support under the grant NSC88-2216-E-007-032.

1) M. Terao: Proc. SPIE **1078** (1989) 2.
2) D. Strand and D. Alder: Proc. SPIE **420** (1983) 200.
3) R. H. Liu: Master thesis of the Department of Materials Science and Engineering, National Tsing Hua University, Taiwan, R.O.C., 2000.
4) C.-Y. Liu: Master thesis of the Department of Electro-optical Engineering, National Chiao Tong University, Taiwan, R.O.C., 1996.
5) R. Zallen: The Physics of Amorphous Solids (1985) p. 98.
6) S. R. Ovshinsky: J. Non-Cryst. Solids **141** (1992) 200.
7) G. M. Pharr and W. C. Oliver: J. Mater. Res. **7** (1992) 1564.